Liquid Crystals
Publication details, including instructions for authors and subscription information:
http://www.informaworld.com/smpp/title~content=t713926090

Modelling of shear flow in liquid crystalline materials

M. S. Lavine; A. H. Windle

Online publication date: 06 August 2010

To cite this Article Lavine, M. S. and Windle, A. H.(1999) 'Modelling of shear flow in liquid crystalline materials', Liquid Crystals, 26: 10, 1521 — 1530
To link to this Article: DOI: 10.1080/026782999203850
URL: http://dx.doi.org/10.1080/026782999203850

LIQUID CRYSTALS, 1999, VOL. 26, NO. 10, 1521–1530

Modelling of shear flow in liquid crystalline materials

M. S. LAVINE† and A. H. WINDLE*

Department of Materials Science and Metallurgy, University of Cambridge, Pembroke Street, Cambridge CB2 3QZ, England

(*Received 21 May 1998; in final form 4 May 1999; accepted 14 May 1999*)

The flow behaviour of liquid crystalline polymers (LCPs) is quite complex and these materials exhibit varied and complicated textural patterns when subject to a flow field. The complexity arises from two general factors, the first that they are long chained and thus have long relaxation times, and second that they are liquid crystalline, and thus there is co-operative motion of the molecules. In both thermotropic and lyotropic LCPs subject to low shear flows, it is known that defects and disclinations influence the microstructure and rheology, but it is not clear by what mechanisms these distortions shrink or multiply during flow. In this work, a model is developed to examine the behaviour of defects in shear flows. The simulations based on the model show a spectrum of microstrucural development as a function of applied shear rate: reorientation of domains of different alignment associated with disclinations at low shear strains; the multiplication of wall type defects and the orientation of these normal to the shear gradient axis at intermediate shear rates, and the tendency towards disclination annihilation; the generation of a flow-aligned monodomain at higher shear rates.

1. Introduction

A shear field, with its extensional and rotational components, is one of the more complicated fields which can be applied to liquid crystalline materials. In the case of small molecule nematics, such as those used in display devices, the orientation of the director is influenced by both components of the shear. While it is possible to predict the response of a monodomain to such a field, even where boundary conditions are also contributing to the total effect, the presence of disclination-type defects (topological singularities) greatly complicates the behaviour. There are the issues of possible disclination multiplication in shear, their removal by normal 'annealing' processes, the generation of additional distorted regions and finally the possibility of shear driven conversion of defect-containing structures to monodomains aligned in the shear (velocity) direction.

Liquid crystalline polymers generally have longer relaxation times, so that any process by which defects are removed from a sample, whether under the influence of external fields such as shear or not, will be slower and the achievement of a monodomain more difficult. The processing of liquid crystalline polymers, although remarkable in the level of molecular alignment which can be achieved for comparatively modest flows, seldom leads to samples which have perfect monodomain structures. The defects cannot but influence the final properties. However, there is also evidence, at least in thermotropic systems, that the oriented liquid crystalline polymer contains a molecular network-type memory of its extension during processing, such as is typical of conventional (flexible chain) polymers. The presence of such a network has retractive consequences where the polymer is heated above its glass transition temperature. The modelling reported here does not extend to the consideration of the viscoelastic properties of the material either during shear or on stress relaxation. It takes the first step of understanding the complex consequences of shearing a liquid crystalline sample containing defects over a range of strain rates. It addresses the polymeric case insofar as examining the influence of non-equal Frank constants (specifically a high splay constant) on the simulation.

*Author for correspondence.

†Now at the Department of Chemical Engineering, MIT, Cambridge, MA 02139, USA.

2. Historical

A detailed study on the microstructural influence of a shearing flow on a small molecule liquid crystal and a molecular mass series of thermotropic liquid crystalline polymers (LCPs) was first performed by Graziano and Mackley [1, 2]. Their studies found that there were parallels in the observed textures between the two types of material which were unique to liquid crystalline materials. There were also some striking differences between the two materials which were attributed to the much longer relaxation times of the liquid crystalline polymers.

Journal of Liquid Crystals ISSN 0267-8292 print/ISSN 1366-5855 online
http://www.tandf.co.uk/JNLS/lct.htm
http://www.taylorandfrancis.com/JNLS/lct.htm

During the experiments on MBBA, a conventional liquid crystal [1], the glass surfaces were treated to promote homeotropic anchoring. At low shear rates the molecules flow-aligned without forming defects, with the extent of alignment determined by the balance between surface driven and flow based forces. At higher shear rates, both half strength singular lines and integer strength, escaped lines were observed. The former were seen as thin threads whose appearance was independent of the polarization angle of the incident light, while the latter were thicker in appearance and sensitive to the polarization angles. Both were observed as forming closed loops.

During shear, the loops (both thick and thin) were seen to elongate, deform and tumble as a result of the velocity gradients acting across them. The density of loops increased with increasing shear rate until the field of view was full of a tangled defect network. In contrast with static observations of the same loops they were much narrower, indicating that the director distortions were compressed and localized by the flow.

On cessation of shear the closed loops were seen to collapse. The relaxation processes were much slower than the restoration of the bulk homeotropic alignment to the rest of the sample, i.e regions far from the disclinations quickly aligned with the boundary orientation, while the disclination network slowly relaxed.

The observations of the thermotropic LCP system [2] showed some similarities to the small molecule observations, but also some features unique to LCPs, and these differences were attributed to the lower molecular mobilities of the polymers.

For the polymer with the lowest molecular mass, a number of textures were observed during shear. At low shear rates, the disclination lines multiplied dominating the entire field. At higher shear rates, the lines gave way to dark, curled entities which continually changed shape, forming what was termed a 'worm texture', but no physical explanation was provided other than that it represents a disclination texture too fine in detail to be resolved optically. At even higher shear rates the details of any defect lines were lost and a quasi-monodomain texture formed which was called an 'ordered' texture, and which had maximum optical extinction when the crossed polarizers were aligned at 0° and 90° to the flow direction.

For a polymer with a much higher molecular mass [2], the quiescent sample showed a worm texture. This texture was only stable at very low shear rates, and at no stage were the thread or line textures observed. At low shear rates the sample adopted the ordered texture, which was the dominant texture for this material.

A survey of the literature by Graziano and Mackley [2] found supporting evidence that the textures that they had observed had also been seen in a wide range of LCPs, including lyotropics, but not in isotropic polymer melts and solutions, or in small molecular nematics. The wide ranging occurrence of these textures suggested that they were due to the specific intermolecular ordering of the LCPs and were not a function of the specific chain structure and chemistry (although these factors will influence the stability of the liquid crystalline phase between one LCP and another). The two factors which seemed to induce the textures were the comparative rigidity of the molecules (not present in isotropic polymers), and the long molecular length which increased the molecular relaxation times. Such textures have also been seen in lyotropics and appear to be a characteristic of the LCP state. There is also experimental evidence that an increase in the molecular mass of the LCP or a decrease in the temperature produced the same effect on the texture as an increase in the shear rate.

3. Theoretical background

The distortion free energy, per unit volume, is [3]

$$F_d = \frac{1}{2}[K_{11}(\nabla \quad \mathbf{n})^2 + K_{22}(\mathbf{n} \quad \nabla \times \mathbf{n})^2 + K_{33}(\mathbf{n} \times \nabla \times \mathbf{n}^2] \tag{1}$$

where K_{11}, K_{22} and K_{33} are the (Frank) elastic constants associated with the splay, twist and bend distortions respectively.

The distortion energy is minimized when all the directors uniformly align, i.e. when they form a monodomain. Often the attainment of a monodomain is not possible due to non-uniform influences at the boundary conditions, and it is also less likely to be achieved when liquid crystals are cooled rapidly through the isotropic–nematic transition.

Any non-uniformity in the director field is known as a distortion, and will increase the free energy of the system. If the director field undergoes a large change within a localized yet comparatively isolated region, then it tends to be known as a defect, and if the defect contains a topological singularity at its core region then it is known as a disclination [3]. Examples of defects are shown in figure 1 which is a simulation of a slice through a disclination loop. Two disclinations can be seen in the image, a + 1/2 at the top and a – 1/2 below it. The strength of a disclination can be determined by tracing a 2π circuit around the centre of the defect: for 1/2 strength disclinations, the angle that the director makes with some fixed reference direction will change by π. For positive signed disclinations the director and the circuit follow the same direction, while for negative signed disclinations they will be of opposite direction. Between the two disclinations the director can be seen

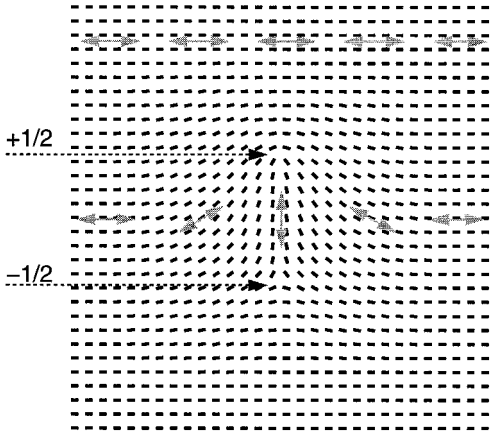

Figure 1. The centre slice through a disclination loop shows the + 1/2 and – 1/2 wedge disclinations. The line singularity of the loop is coming out of the plane of the page at the + 1/2 disclination and going back into the page at the – 1/2 disclination.

to rotate by π as one travels from left to right, as highlighted by the grey double arrows. This sort of defect is known as a wall, the centre of which is the disk bounded by the disclination loop. Wall defects by themselves are not stable and will relax out to give a monodomain of uniform orientation, but they can be stabilized by other defects (a disclination loop in this example) or by external fields.

4. Model

The model consists of a lattice of cubic cells, each of which contains a director (**n**) of the average local orientation, which is described by a unit vector, or more accurately pseudo-vector, as $\mathbf{n} = -\mathbf{n}$. Each director represents the average orientation of a large number of molecules or of a certain spatial neighbourhood, as illustrated in figure 2; this model is thus not operating on a molecular scale.

The centres of the directors are confined to the sites of a cubic lattice, while their orientation is allowed to vary in three dimensions. The boundary conditions of the lattice can be set to mimic the physical system that is being simulated: periodic boundary conditions are used to make the lattice represent the bulk, fixed boundary conditions are used to represent specific wall orientations,

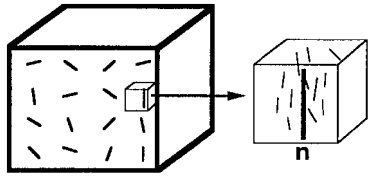

Figure 2. A nematic is divided into a lattice of cubic cells. The average orienation of the molecules within each cell is represented by a local director **n**, where $\mathbf{n} = -\mathbf{n}$.

and free boundary conditions are used if the sample is not confined or influenced by its surroundings. Different boundary conditions can be used, e.g. a mixture of fixed and free boundaries to simulate a nematic placed between two cover slips.

In the model used for the initial shear studies reported here, the distortion free energy (equation 1) is approximated by

$$\frac{K}{2}\sum \sin^2(\Delta\theta) \tag{2}$$

where $\Delta\theta$ is the angle between the central and neighbouring directors, K is the one Frank constant, and the summation is performed over nearest neighbours. Details on the choice of this simple energy function and its advantages can be found elsewhere [4, 5]. For the simulations discussed here, the energy function has been differentiated with respect to changes in $\Delta\theta$, in order to calculate the net torque (Γ) acting on the central director. From this the rate of rotation of the director is calculated given the rotational viscosity of the material (η)

$$\dot{\mathbf{n}}_{\text{relaxation}} = \frac{\Gamma}{\eta} \tag{3}$$

When the three Frank constants were allowed to vary, a first order weighting function was used, similar to the one of Bedford and Windle [4], to separate the splay and bend fractions of a distortion, as these are intrinsically linked when using a fixed position lattice model.

The response to the flow is incorporated using Ericksen's theory [6, 7] for transversely isotropic fluids. The theory describes the response of an isolated director to an applied flow field, based on the applied shear rate, where the rate of change of the director is given by

$$\dot{\mathbf{n}}_{\text{shear}} = \mathbf{n}\ \ \omega + \lambda(\mathbf{n}\ \ \mathbf{A} - \mathbf{A}:\mathbf{nnn}) \tag{4}$$

where **A** is the strain rate tensor, ω is the vorticity tensor, and λ is an orientation shape parameter which can be used to describe the extent of the correlation between the motion of the individual molecules and the director, and determines the balance between the rotational and elongational components of the simple shear in determining the director response.

When λ is set to unity, the equation describes affine rotation, in that a line drawn on the surface of the shearing solid which lies parallel to the velocity and the velocity gradient axes, rotates on shearing as described by the equation. It predicts that for large extensions the director will tend towards the velocity axis to give 'flow alignment'. The particularly strong intermolecular orientational coupling in thermotropic liquid crystalline polymers suggests that unity is an appropriate value for λ, and all the modelling reported below is carried out with this setting.

However, to argue for $\lambda = 1$ it is necessary to explore the meaning of different values in an experimental context. When $\lambda = 1$, an exact balance between the rotational component and the elongationally driven alignment towards the direction at 45° to the flow axis (in the opposite rotational sense) is achieved. Any rotation beyond the exact flow aligning orientation, will immediately lead to further rotation as the rotational component will then dominate. The exact flow aligning orientation is thus only a metastable state.

For values $0 < \lambda < 1$, the rotational component—the first right hand term of (4)—dominates, and the equation will predict a continuous rotation of the director with on-going shear deformation. This class of behaviour is known as the tumbling regime. Tumbling behaviour occurs when thermal disturbances enable a small nucleus of molecules to rotate 'over-centre' and progressively drag more material over with it. Tumbling behaviour has been observed in several lyotropic liquid crystalline systems [8]. In the case where $\lambda > 1$, the prediction is of a stable flow alignment, but in this case the angle made to the velocity axis is not zero and increases with λ. It is know as the Leslie angle [9]. The orientation settles to between the velocity and (45°) extensional axes. The reason why such behaviour may be observed can be understood by considering such systems where the mutual attraction of neighbouring molecules is on the same scale as the thermal fluctuations, such as in some small molecule nematics. There will be a considerable molecular thermal distribution of the long axis of the molecules about the director, giving rise to values of the order parameter considerably below unity. In this case molecules which are thermally kicked over the velocity axis 'centre' will rotate on their own to give a reorientation of approximately π. The result is that the orientation distribution will not peak on the velocity axis, but at some angle 'before' it, as the components of the distribution closer to it are continually being thermally rotated over and away.

The choice of $\lambda = 1$ for the simulation of thermotropic liquid crystalline polymer systems follows from the understanding that it is unlikely that a given molecule will rotate independently of its neighbours. The high level of neighbouring orientational coupling of these materials is reflected in measurements of the local order parameter which approach unity [10] and the fact that in many cases the observations are made several hundred degrees below T_{NI}. The influence of values of λ less than unity in forcing tumbling has not yet been explored. At this stage we are particularly interested in tumbling which results from the influence of defects (see below) and thus do not wish to introduce it into the model through the device of setting λ less than unity.

In summary, at each iteration three calculations are made on each of the cells of the lattice. They are of:

(1) the net distortion torque to determine the relaxation of the director;
(2) the net rotation of the director due to the shearing of that cell;
(3) the macroscopic motion or translation of the fluid element as a function of its position in the lattice.

This last calculation arises from the motion of one layer relative to that above and below it as measured along the velocity gradient direction. In the model, this is accomplished by translating the orientation of a cell's director to the next cell in the flow direction, when the shear strain of that cell has increased by the dimension of the cell.

The overall process is thus an iterative solution towards the torque balance acting on each of the fluid elements.

Although it may seem contradictory to use a lattice model to represent a nematic liquid crystal which does not exhibit positional ordering, such models were first successfully used by Lebwohl and Lasher [11] to study the nematic–isotropic transition. More recently their model has been modified by Ding and Yang [12–14] to include Brownian dynamics for the investigation of rheology and textural changes during flow. From their simulations they were able to reproduce many of the transient phenomena seen experimentally, such as damped stress oscillations and negative first normal stress difference at moderate shear rates. The success of these models lies in the representation of a cluster of molecules by a single vector or director of local orientation, so that the lattice does not, in effect, impose any artificial ordering on the nematic. In this work the scale of the director has been increased considerably in order to examine the shear behaviour of disclinations, although the potential exists for scaling the size of the lattice as required.

One final assumption that has been made is that there is a uniform shear rate across the sample. This implies that each cell will have its own contribution to the overall shear stress, and that each cell will experience a different stress. The alternative and opposite extreme is to consider a uniform shear stress, with variations in the shear rate between different domains [15]. In the linear limit of the Doi theory, these two extremes have been shown to give upper and lower bounds in calculations of viscous stress contributions [16], with only a small range between the two limits, and so the constant shear rate approach is a reasonable approximation to make.

5. Results

The behaviour of a textured sample was simulated over a range of shear rates. The simulations reported

here were run for the same total strain ($\gamma = \dot{\gamma}t$), using a common initial lattice. A single slice three dimensional lattice (of size $100 \times 100 \times 1$ cells, not including the boundaries) was chosen so that individual disclinations could be followed with time, and the directors would also be able to tilt out of the shear plane. (In this work the shear plane is defined as the velocity–velocity gradient plane, although some researchers define the shear plane as the velocity–vorticity plane.) Fixed homeotropic top and bottom boundary conditions were used, in order to prevent the escape of disclinations which would otherwise occur with free boundaries, and because they are the most commonly used boundary conditions in experimental studies. For all the simulations, the cell size was set at 100 nm, the Ericksen shape parameter λ was set to unity, and the rotational viscosity to 1.0 Pa s. Except for the last result presented, a single Frank constant was assumed with a value of $K = 1 \times 10^{-11}$ N.

One way of comparing the observations from different materials is through the use of dimensionless parameters. For liquid crystalline materials, the most commonly used parameter is the Ericksen number (Er) which gives the ratio of the viscous forces to the elastic forces, and is given by the formula

$$Er = \frac{V d \gamma_1}{K} \tag{5}$$

where V is the velocity of the moving surface, d is the sample thickness or gap width, γ_1 is the rotational viscosity, and K is the characteristic or average Frank constant. There does not appear to be a standard definition for K, and it is either set as K_{11} or K_{33}, whichever is deemed more representative for the material in question, or the three constants are averaged [17]

$$K = (K_{11} K_{22} K_{33})^{1/3}.$$

The Ericksen number can also be written in terms of the shear rate $\dot{\gamma}$,

$$Er = \frac{\dot{\gamma} d^2 \gamma_1}{K}. \tag{6}$$

Thus for the single Frank constant simulations, $Er = 10\dot{\gamma}$.

Two limitations of the simulation conditions are worth noting. Although the lattice is 100 cells high, it only represents a thickness of 10 μm, which is smaller than the samples used in most experimental flow studies; the homeotropic boundaries will thus have a stronger influence than they do experimentally. It is still the best choice of boundary condition though, as any other fixed boundary might confuse the director changes caused by the flow. The second consideration is that while the directors have full three dimensional orientational freedom, it is not possible for disclination lines to form parallel to the velocity gradient direction, due to the study of a single layer in the vorticity direction. This simplification also means that the disclinations present in the sample very probably have more mobility than if they were part of fully three dimensional lines.

The starting structure for all the simulations was the same 'partially relaxed' structure containing a number of disclinations. It is shown in figure 3. The colours are used to indicate the director orientation with pure blue in the flow (velocity) direction, pure green in the velocity gradient direction and pure red in the neutral or vorticity direction. The disclinations are highlighted at their core regions by the small boxes which are located at the cells with the highest distortion energy. There are three pairs of $\pm$ 1/2 wedge disclinations, although the pair near the top left corner are difficult to identify because of their twisting out of plane. Between each pair of disclinations exists a highly delocalized wall defect, which marks a region where the director angle changes quickly over a short distance. The boundary conditions at the top and bottom of the model were set to homeotropic.

Shear rates covering five decades between 0.1 and 1000 s^{-1} were studied, covering Ericksen numbers 1 to 10 000. Each of the simulations was run for 200 strain units in total ($\gamma = \dot{\gamma}t$). At the lower extreme ($\dot{\gamma} = 0.1\ s^{-1}$) the behaviour was similar to that at a shear rate of 1.0 s^{-1}, except that the homeotropic boundaries were even more dominant. For $\dot{\gamma} = 1\ s^{-1}$, shown in figure 4, the boundary orientation permeates through the structure, and would do so through its entirety, except for the presence of the disclinations which separate the boundary-dominated orientation from one which aligns with the flow direction. The disclinations move past each other but are not seen to attract each other strongly enough to combine and annihilate. Also, the flow is not fast enough to cause the + 1/2 disclinations to reorient, while the – 1/2 disclinations continuously spin. Thus it is possible that when they approach each other, they are not aligned in a way which would be conductive to their attraction and annihilation, which has been shown to be an initial step for defect pair annihilation [18]. The vectors can also be seen to move further into the shear plane (defined as the plane of the page), as evidenced by the loss of any red colour.

At a shear rate of 10 s^{-1} a number of different observations can be made from the images shown in figure 5.

The first is the reduction in the amount of green, as the faster flow reduces the influence of the boundary conditions to a thin boundary layer of 4–8 cells. The bulk of the vectors are mainly blue in colour, indicating good alignment with the flow direction, except for wall distortions which lie between pairs of disclinations. The walls are narrow and better defined than at lower strain rates. Across the walls, the vectors can be seen to rotate

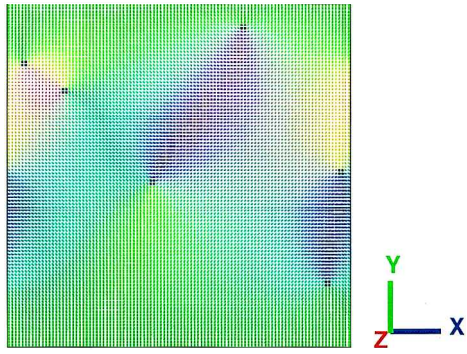

Figure 3. Starting condition for the thin slice simulations.

by 180°. The reorientation occurs not only in the shear plane, but also out of the plane, as shown by the red region between the bottom pair of disclinations.

The shear rate is fast enough so that the + 1/2 disclinations are also seen to rotate about their rotation axes, and between the simulation at strain 100 and strain 150, two pairs of defects have attracted each other, merged and annihilated. The decrease in the total number of disclinations reduces the amount of material which is able to remain twisted out of plane, and by a strain of 200 the bulk of the vectors are aligned with the flow direction.

At a shear rate of 100 s^{-1} the annihilation of two of the pairs of disclinations occurs at lower strain, with only one pair remaining by a strain of 100 as seen from the images shown in figure 6. The texture, however, is quite different from the previous case, and is dominated by regions that are aligned with either the flow or vorticity directions. Between strain 150 and 200, a pair of disclinations was seen to emerge from an area of high distortion and interact with the existing disclination. In this shear rate regime, there is thus evidence for the multiplication of wall area, and the orientation of the walls parallel to the vorticity/velocity plane. The walls are essentially twist in character and rotate and otherwise flow aligned orientation through the vorticity direction at the wall centre.

At a shear rate of 1000 s^{-1} the disclinations are very rapidly destroyed. Figure 7 shows two comparatively low strain views ($\gamma = 5$ and 50). At $\gamma = 50$ we have just two walls without termination at disclinations (they are of course tesselated horizontally by the periodic boundary conditions in that direction). Such behaviour is not unexpected as it can be argued that as the strain rate increases towards infinity, then the shear-induced field will totally dominate over the nematic field and all directors will simply respond to the dominant field and flow align with the velocity axis, thus removing

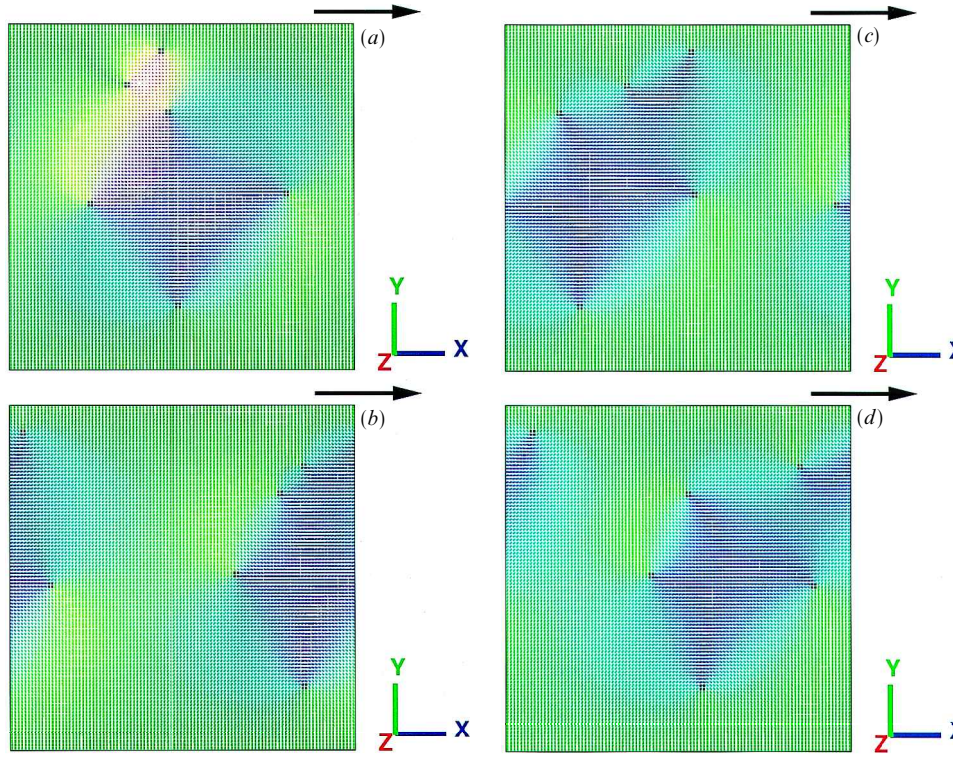

Figure 4. Shearing of a thin slice, $\dot{\gamma} = 1.0\ s^{-1}$, $\gamma =$ (*a*) 50, (*b*) 100, (*c*) 150 and (*d*) 200. The arrow shows the flow direction of the upper surface of the lattice.

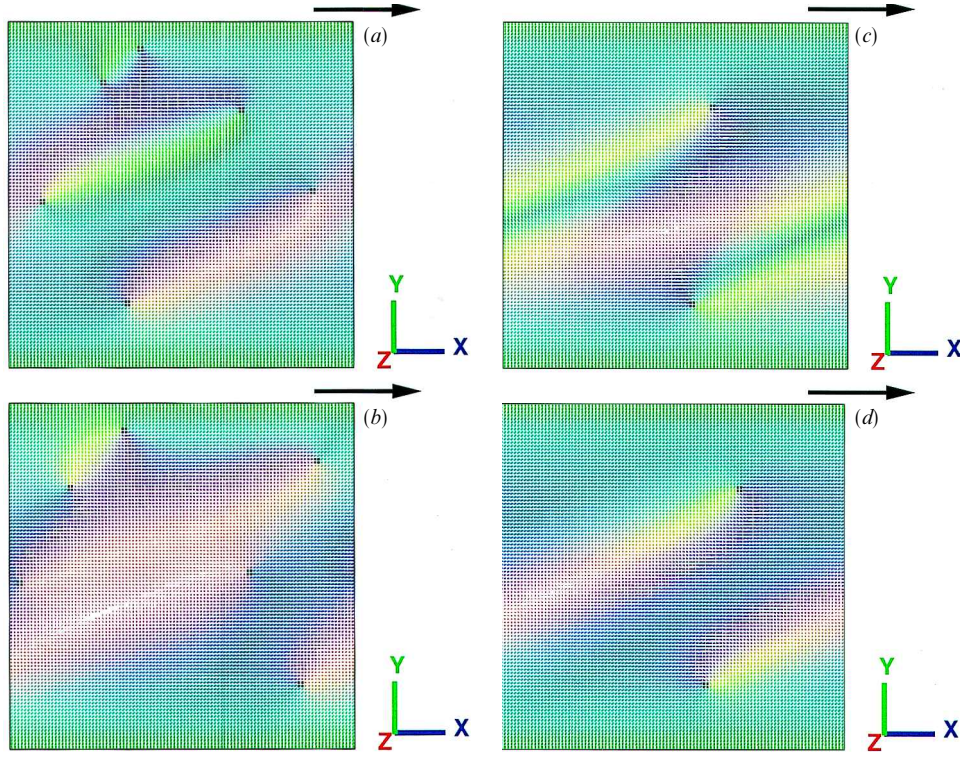

Figure 5. Shearing of a thin slice, $\dot{\gamma} = 10.0\ s^{-1}$, $\gamma =$ (*a*) 50, (*b*) 100, (*c*) 150 and (*d*) 200. The arrow shows the flow direction of the upper surface of the lattice.

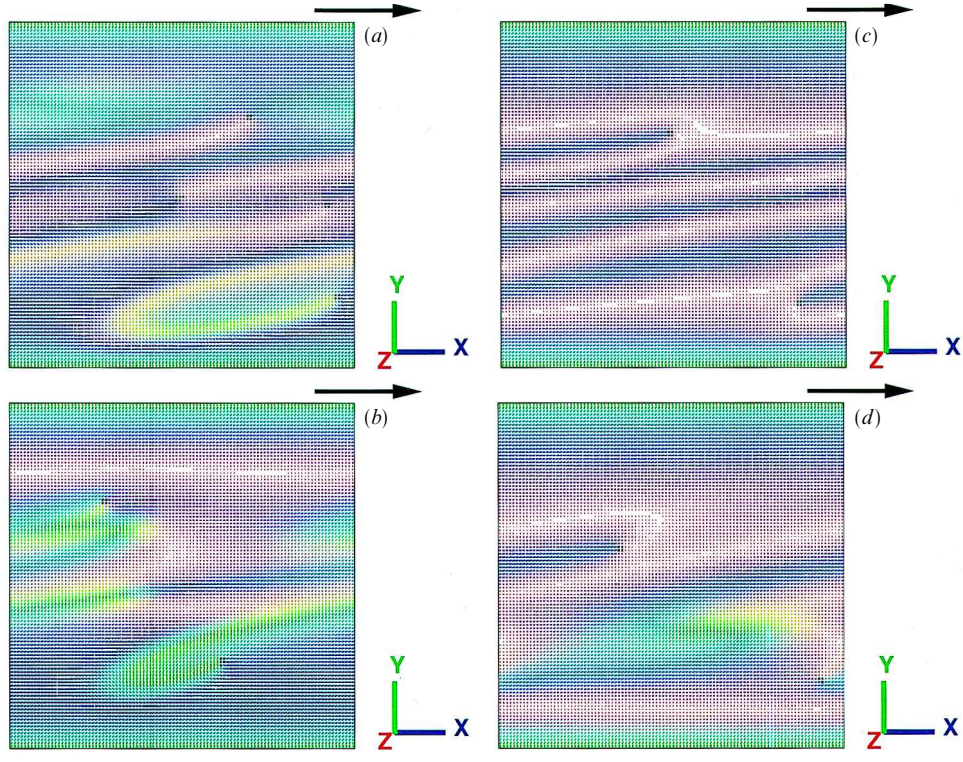

Figure 6. Shearing of a thin slice, $\dot{\gamma} = 100.0\ s^{-1}$, $\gamma =$ (*a*) 50, (*b*) 100, (*c*) 150 and (*d*) 200. The arrow shows the flow direction of the upper surface of the lattice.

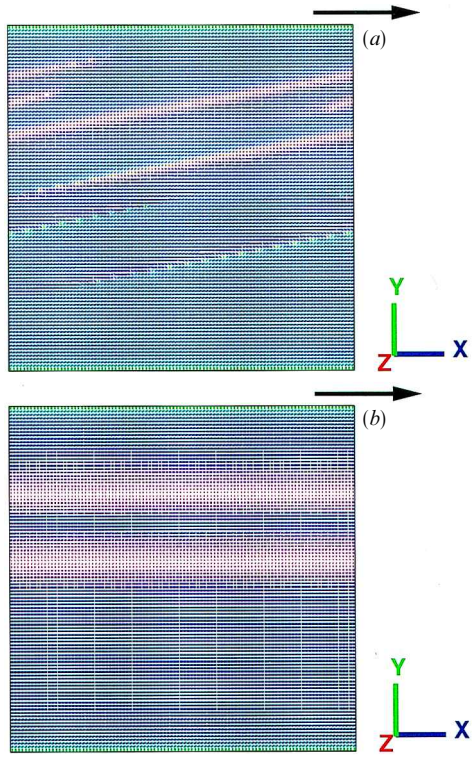

Figure 7. Shearing of a thin slice, $\dot{\gamma} = 1000.0\ s^{-1}$, $\gamma =$ (*a*) 5 and (*b*) 50. The arrow shows the flow direction of the upper surface of the lattice.

defect structures and generating a perfect monodomain. Whether disclinations can actually be eliminated in this way in practice remains to be seen.

5.1. *High splay simulations*

A few simulations were run with unequal elastic constants, and in particular with the splay constant five times greater than twist and bend constants (i.e. $K_{11} = 5 \times 10^{-11}$ N and $K_{22} = K_{33} = 1 \times 10^{-11}$ N). The ratio of these values is more characteristic of a thermotropic LCP. Raising the splay constant has two effects, it increase the elastic stresses relative to the viscous, but at the same time, by making the constants unequal, there are more restrictions placed on the motions of the director as those orientations which cause a large amount of splay distortion are now not favoured.

The results for one of the simulations is reported here, for a shear rate of $100\ s^{-1}$, corresponding to an Ericksen numbers of 585 (where the characteristic Frank constant used to calculate Er is equal to the cube root of the product of the three K_{ii} [17]). The Ericksen number lies between that calculated for the equal constant simulations for shear rates of 10 and $100\ s^{-1}$ and one would expect that the behaviour should show some similarity to these results.

The results for the simulation with $\dot{\gamma} = 100\ s^{-11}$ are shown in figure 8.

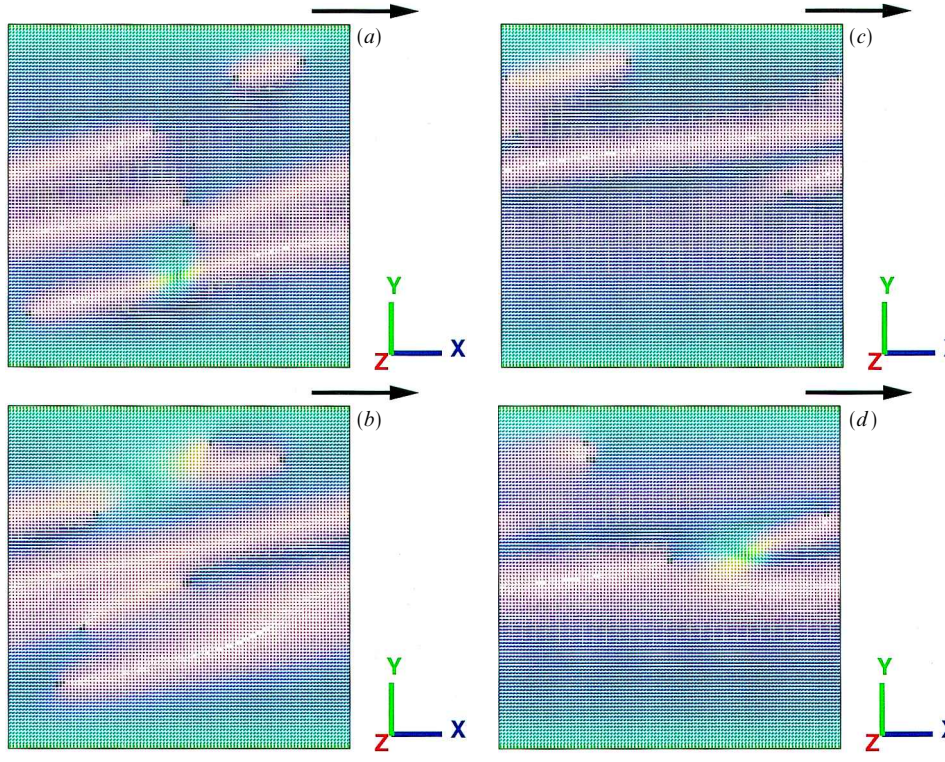

Figure 8. High splay shearing of a thin slice, $\dot{\gamma} = 100.0\ s^{-1}$, $\gamma =$ (*a*) 50, (*b*) 100, (*c*) 150 and (*d*) 200. The arrow shows the flow direction of the upper surface of the lattice.

At this shear rate, the behaviour is similar to that observed for the same rate with the equal elastic constants. The vector field is dominated by regions of blue and red. The boundary layer has been reduced to only a few cells thick, which is consistent with experimental observations.

6. Discussion

The simulations suggest a hierarchy of shear-induced structural development which depends on strain rate.

The model is arguably the most simple of its type possible and is seen as the best first step in an on-going modelling programme to simulate the structures of thermotropic liquid crystalline polymers under processing conditions. The model is simple in that: (1) the equal Frank elastic constant approximation is used in most of the work, (2) the model is in effect ultra-thin in the vorticity direction with periodic boundary conditions operating (a 2.5 dimension approximation) and (3) the constant in the equation derived from Ericksen (λ) is set to unity so that the predicted orientation changes in the directors are affine with the bulk deformation. The model does not attempt to simulate viscoelastic properties of the medium, which are likely to be significant for polymeric materials.

Although simple, the model shows a number of significant phenomena which begin to add understanding to the relevant experimental observations already reported.

Disclinations of strength 1/2 (the only type seen in these models and considered here) respond to a shear field in different ways. As previously reported [19], they appear to rotate about the vorticity axis, the sign of the strength of the defect determining the sense of the rotation; the rotation is associated with the multiplication of wall type defects.

The model demonstrates that at low shear rates, less than approximately 10 s^{-1} (c.f. figure 4), the regions of orientation distribution which represent the local (internal) field of the disclinations are not destroyed by the application of shear deformation. Instead, the regions rotate with the vorticity of the field and there is little development of overall orientation in the structure. As would be expected, the homeotropic boundary conditions have a considerable influence in such modest flows and the boundary-induced orientation propagates significantly into the model where it is not disrupted by the disclination fields. When a similar model is run in a full three dimensions, the extensional aspect of the shear draws out disclination lines and thus the overall disclination density would be expected to increase. Such predictions would correspond to the Graziano and Mackley observations of shearing liquid crystals and liquid crystalline polymers at low strain rates.

At higher strain rates the localization of walls becomes more prominent and their total area increases as the disclinations are moved apart by the flow. There is also evidence that as the distorted areas begin to interact, disclination pairs form as a means of relieving the distortion, a mechanism first proposed by Marrucci [20]. Walls are more compact at higher strain rates as a consequence of the increasingly strong orientational field which will minimize the amount of material which is thus not aligned (figure 5). The generation of walls and their tendency to rotate near to their bounding disclinations, will have significant and as yet unmodelled effects on the optically observed microstructures. However, the essentially twist character of the walls lying in the velocity/vorticity plane will rotate the plane of polarized light and are thus likely to have a significant disruptive influence on the optical texture. Nevertheless, we wish to record that the generation and interaction of such wall-like distortions may provide a possible explanation of the worm textures reported by Graziano and Mackley.

As the strain rate is increased towards 100 s^{-1} the walls become more extensive and lie parallel to the vorticity/velocity plane (figure 6). At higher strain rates they appear to become less numerous and especially thin, in response to the increasing influence of the applied flow-aligning field. The optical microstructures of such structures, as viewed in the velocity gradient direction (vertical in the simulations displayed here), would probably be indistinguishable from a monodomain, again in accord with the experimental results.

The comparatively modest effect on the predicted structures of increasing the splay elastic constant to five times that of the twist and bend, is interesting to note and suggests that in shear flow, as opposed to quiescent structures, different constants may have a relatively minor influence, the main effect being in the way the disclination networks are able to relax. It should be noted however, that the relatively low twist constant of polymeric structures would tend to encourage further the dominant twist character of the walls generated under equal constant simulations.

7. Conclusions

A computational model has been built and run which simulates the influence of shear flow on the microstructure of liquid crystalline polymers. It is run for a wide range of strain rates, in each case with the same starting structure and boundary conditions.

For the affine modelling of the rotational component of shear ($\lambda = 1$) the simulation has been run over a range of strain rates from 0.1 to 1000 s^{-1}. At strain rates below 10 s^{-1} the starting structure rotates and becomes displaced within the shear field. There are few qualitative changes with increasing strain. The orientation at the

boundary dominates the texture, except at regions near the disclinations.

In the strain rate range spanning 10–100 s^{-1} the shear gives rise to an increased density of wall-type distortions. There is some rotation of these distorted regions close to their bounding disclinations.

With further increase in strain rate, the walls become parallel to the velocity/vorticity plane, thinner and possibly less frequent, as most of the structure assumes the flow-aligning orientation.

The sequence of structural predictions maps onto previous experimental observations, and it is suggested that the generation of multiple walls may be the origin of the 'worm' texture described by Graziano and Mackley.

The introduction of a splay constant five times larger than the twist and bend constants, does not greatly affect the behaviour under shear, but it does reduce the relaxation rate of the distorted areas after the cessation of shear-flow.

References

[1] Graziano, D. J., and Mackley, M. R., 1984, *Mol. Cryst. liq. Cryst*., **106,** 73.

[2] Graziano, D. J., and Mackley, M. R., 1984, *Mol. Cryst. liq. Cryst*., **106,** 103.

[3] Frank, F. C., 1958, *Discuss. Faraday Soc*., **25,** 19.

[4] Bedford, S. E., and Windle, A. H., 1993, *Liq. Cryst*., **15,** 31.

[5] Assender, H. E., and Windle, A. H., 1994, *Macromolecules*, **27,** 3349.

[6] Ericksen, J. L., 1960, *Arch. ration. Mech. Anal*., **4,** 231.

[7] Ericksen, J. L., 1960, *Z. Kolloid*, **173,** 117.

[8] Burghardt, W. R., and Fuller, G. G., 1990, *J. Rheol*., **34,** 959.

[9] Larson, R. G., 1988, *Constitutive Equations for Polymer Melts and Solutions*, Butterworth Series in Chemical Engineering (Boston: Butterworth).

[10] Donald, A. M., and Windle, A. H., 1992, *Liquid Crystalline Polymers*, Cambridge Solid State Science Series (Cambridge: Cambridge University Press).

[11] Lebwohl, P. A., and Lasher, G., 1972, *Phys. Rev. A*, **6,** 426.

[12] Ding, J., and Yang, Y., 1994, *Rheol. Acta*., **33,** 405.

[13] Yang, Y., and Ding, J., 1994, *Macromol. Symp*., **87,** 115.

[14] Ding, J., and Yang, Y., 1995, *Macromol. Symp*., **96,** 135.

[15] Marrucci, G., and Maffettone, P. L., 1990, *J. Rheol*., **34,** 1217.

[16] Cocchini, F., Aratari, C., and Marrucci, G., 1990, *Macromolecules*, **23,** 4446.

[17] Han, W. H., and Rey, A. D., 1995, *J. Rheol*., **38,** 1317.

[18] Shiwaku, T., Nakai, A., Wang, W., Hasegawa, H., and Hashimoto, T., 1995, *Liq. Cryst*., **19,** 679.

[19] Lavine, M. S., and Windle, A. H., 1997, *Macromol. Symp*., **124,** 35.

[20] Marrucci, G., 1991, *Macromolecules*, **24,** 4176.